

High-Resolution Scanning Tunneling Microscopy Images of Molecular Overlayers Prepared by a New Molecular Beam Deposition Apparatus with Spray-Jet Technique

Toshiki Yamada,* Hitoshi Suzuki, Hideki Miki, Ge Maofa,[†] and Shinro Mashiko

Kansai Advanced Research Center, National Institute of Information and Communications Technology, 588-2 Iwaoka, Kobe 651-2492, Japan

Received: August 11, 2004; In Final Form: October 6, 2004

We developed a new molecular beam deposition apparatus using a spray-jet technique for high-quality thin film preparation of nonsublimable molecules. The apparatus was used to deposit chloro[tri-*tert*-butyl-subphthalocyaninato]boron(III) (TBSuPc) molecules on an Au(111) surface for analysis by low-temperature scanning tunneling microscopy (STM). Highly resolved images, in which *tert*-butyl groups in a TBSuPc molecule were clearly identifiable, were obtained. The image quality and the resolution of these images compared favorably well to STM images taken on reference samples which were sublimed onto Au (111) from a heated crucible.

Introduction

In the past decade, scanning tunneling microscopy (STM) has become one of the most useful tools in surface science. In particular, ultrahigh-vacuum (UHV) STM has produced high-resolution images of many different organic molecules and their overlayer structures on clean substrates.^{1–4} In the majority of the previous studies, the molecules were deposited by thermal evaporation. Recently, functional organic molecules with a medium molecular weight, such as porphyrin, phthalocyanine, and subphthalocyanine derivatives, have been intensively studied using UHV-STM, and researchers have obtained highly resolved images in which the substituents in the molecules are clearly identifiable.^{5–12} These substances with a medium molecular weight used in these previous studies are also thermally stable and evaporable and have attracted a lot of attention because of their potential for molecular electronics.

For nonevaporative molecules, the pulse-injection technique,¹³ which directly injects a sample solution into vacuum through a pulsed nozzle, was developed to deposit molecules on clean metal or semiconductor surfaces. This technique has been used for molecular deposition of macromolecules, such as DNA, RNA, carbon nanotubes, and π -conjugated polymers, and STM images of these materials have been obtained.^{13–16}

Earlier, we developed a spray-jet technique that produces a molecular beam of neutral molecules from the sprayed mist of a sample solution, mainly for use in spectroscopic analysis.^{17–20} This spray-jet molecular beam apparatus consists of: (1) a sample inlet system with an ultrasonic nebulizer, an inlet chamber, and a pulsed nozzle; (2) a set of skimmers; and (3) a high-vacuum chamber in which pulsed-laser photoionization and mass detection are carried out. In the spray-jet technique, a dense mist of the sample solution is first prepared in the nebulizer and then carried with a carrier gas into the inlet chamber, from which a molecular beam is ejected into vacuum through the pulsed nozzle and skimmers.

In the study described here, a new spray-jet molecular beam deposition apparatus was developed to be used in conjunction with STM studies. We chose a subphthalocyanine derivative, a chloro[tri-*tert*-butyl-subphthalocyaninato]boron(III) (TBSuPc), as the test molecule. In our laboratory, we have previously observed highly resolved STM images of TBSuPc molecules deposited on an Au (111) surface by thermal evaporation.¹² Therefore the STM images of TBSuPc molecules deposited using the spray-jet technique can be compared to those obtained after sample preparation by thermal evaporation. TBSuPc is dissolvable in acetone, which is essential for molecular beam deposition using the spray-jet technique. These properties were sufficient to enable us to carry out an initial trial of the suitability of the spray-jet technique to STM investigation. By use of the technique, we obtained STM images of TBSuPc molecules deposited on an Au (111) surface. The quality of the molecular overlayer of the TBSuPc molecules deposited using the spray-jet technique and the deposited spot size are discussed. Finally, some of the features of the spray-jet molecular beam deposition are also discussed, compared to the pulse injection technique.

Experimental Section

Parts a and b of Figure 1 show the chemical structure and molecular model, respectively, of TBSuPc. The molecules have a characteristic triangular and corn-shaped structure with a chloride atom (Cl) on top and three di-iminoisoindol rings around a boron core. It is known that the *tert*-butyl groups in a TBSuPc molecule appear as bright spots in STM images and that TBSuPc molecules tend to adsorb with the Cl pointing toward the substrate.¹²

For the molecular beam deposition, a TBSuPc/acetone solution of 0.5 mM was prepared in a clean room. A special grade of acetone (Wako Pure Chemical Industries, Ltd.) was used as the solvent. The sample solution was filtered through a Teflon filter (0.2 μ m) to eliminate dust particles before it was used in the experiments.

Figure 2 shows a schematic of the spray-jet molecular beam deposition apparatus, which is essentially the same as that previously reported,^{17–20} except that the time-of-flight mass spectrometry (TOFMS) unit used in the previous studies is

* To whom correspondence should be addressed. Phone: +81-78-969-2257. Fax: +81-78-969-2259. E-mail: toshiki@nict.go.jp.

[†] Present address: Center of Molecular Science, Institute of Chemistry, Chinese Academy of Sciences, Beijing 100080, People's Republic of China.

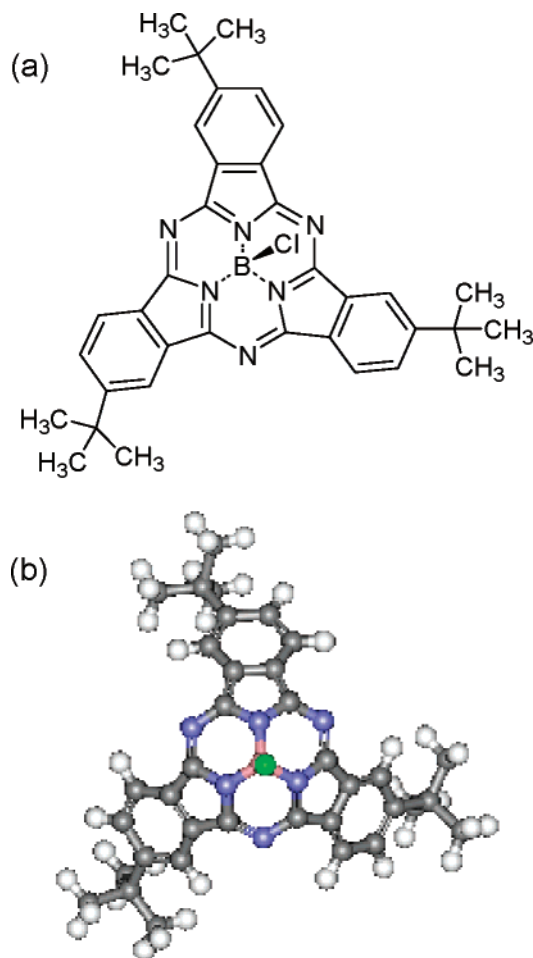


Figure 1. (a) Chemical structure and (b) molecular model of TBSuPc. This molecule has a characteristic triangular and corn-shaped structure with a chloride atom on top and di-iminoisoindol rings around a boron core.

replaced by the UHV chamber shown in Figure 2. The spray-jet inlet system consists of an ultrasonic nebulizer (OMRON, NE-U17, 1.6 MHz), inlet chamber, and pulsed nozzle (Parker Hannifin, 9-279-900). The nebulizer's power and flow controls were adjusted to allow a mist of the solution to enter the inlet chamber. Nitrogen was used as the carrier gas. The inlet chamber, which has a heating unit and drains, is an 80-mm-long stainless steel cylinder with a diameter of 25 mm and an inner volume of approximately 15 000 mm³. The inlet chamber was slightly heated to 45 °C. The orifice of the pulsed nozzle is 0.8 mm in diameter. The distance between the top of the first skimmer cone and the pulsed nozzle was kept to around 5 mm. The distance between the tops of the skimmer cones is 15 mm. The diameter of the holes in both skimmers is 2 mm. The first chamber (A) was evacuated through a liquid-nitrogen trap by a turbo-molecular pump at a pumping speed of 60 L/s; the second chamber (B) was similarly evacuated at 70 L/s. The third chamber (C) was evacuated at 350 L/s by the turbo-molecular pump. The UHV chamber (D), which has a unit for transferring the sample plate to LT-STM (Omicron), was evacuated by a turbo-molecular pump at a speed of 350 L/s and an ion pump with a speed of 110 L/s. The background pressure obtained in the third chamber (C) was 2.6×10^{-6} Pa, and in the UHV chamber (D), it was 8×10^{-8} Pa. The operating time and repetition frequency of the pulsed nozzle were typically 3000 μ s and 5 Hz, respectively. Molecular beam deposition was performed in 300 shots. The pressure in the third chamber (C) typically rose to $1.3\text{--}2.6 \times 10^{-3}$ Pa during the deposition. This

pressure during the molecular beam deposition is about 2 orders in magnitude lower than that during the molecular deposition by the pulse-injection technique.¹³

The substrate for the molecular beam deposition was an Au (111) surface on mica prepared using repeated cycles of Ar sputtering (1 kV) and annealing (~ 710 K) under UHV. The substrate fixed on an omicron sample plate was placed on a manipulator head, usually located at position α in the UHV chamber (D), as shown in Figure 2. When we deposited the molecules, the sample plate was moved to position β in the third chamber. There was a distance of 80–90 mm between the sample plate at position β and the top of the second skimmer cone. After molecular beam deposition, the sample plate was moved back to its previous position α in the UHV chamber. The background pressure in the UHV chamber typically recovered to $3.3\text{--}4.7 \times 10^{-7}$ Pa in 30 min.

We used a commercial UHV-STM system, LT-STM (Omicron) to obtain STM images of the molecules deposited onto the substrate. The system was not directly connected to the deposition apparatus. Therefore, the sample plate was transferred to the LT-STM without breaking the vacuum using the transfer unit, as shown in Figure 2. The sample plate was heated to 450 K to remove residual solvent before the STM measurements. It was then cooled to 77.5 K on the STM stage, and STM measurement proceeded. All the STM measurements were done using a chemically etched W tip at 77.5 K. The base pressure of the STM chamber was kept below 5×10^{-9} Pa during the measurements.

Results and Discussion

In the first process of the spray-jet technique, a mist of solution is prepared by the ultrasonic nebulizer. In the ultrasonic nebulizer, the generation of capillary wave on the solution surface leads to the production of a mist of solution. The average atomized particle size (d (μ m))) is related to the surface tension (T (mN/m)), density (ρ (g/cm³)), and the frequency of nebulizer (f (kHz)). The following formula will help in determining particle size²¹

$$d \approx 190(T/(\rho f^2))^{1/3} \quad (1)$$

In the case of acetone solution, where $T = 23.7$ mN/m and $\rho = 0.785$ g/cm³, the size of the particles centers at 4.2 μ m. In the second process, the mist of solution is carried with a nitrogen gas into the inlet chamber that is slightly heated. The particles can be gas-dried and heat-dried to a smaller size. In the third process, the particles are ejected with a nitrogen gas into a vacuum through the pulsed nozzle and the skimmers. When the particles enter into high vacuum through the pulsed nozzle, the particles are strongly evaporated and fragmented. The fragmentation is further enhanced through the chambers separated by skimmers that are evacuated by the multiple stage differential pumping. Finally a pulsed molecular beam is generated in the third chamber (C). In the molecular beam apparatus as previously described,^{17–20} a pulsed-laser photoionization and mass detection are carried out in the third chamber (C) so as to characterize molecular species in a molecular beam, while in the apparatus as described in the present paper, the spray-jet molecular beam deposition is carried out in the third chamber (C).

First we confirmed the generation of a molecular beam by the spray-jet technique with a TBSuPc/acetone solution of 0.5 mM, using the molecular beam apparatus as previously described.^{17–20} Figure 3 shows a resonantly enhanced multipho-

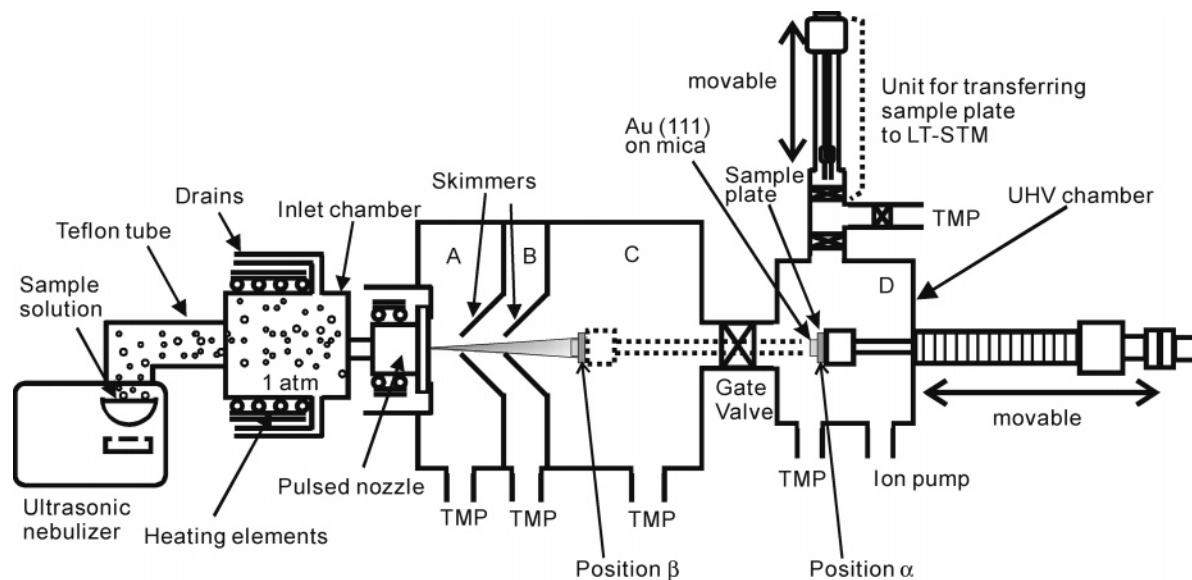


Figure 2. Schematic diagram of our new molecular beam deposition apparatus with spray-jet technique for use in STM studies.

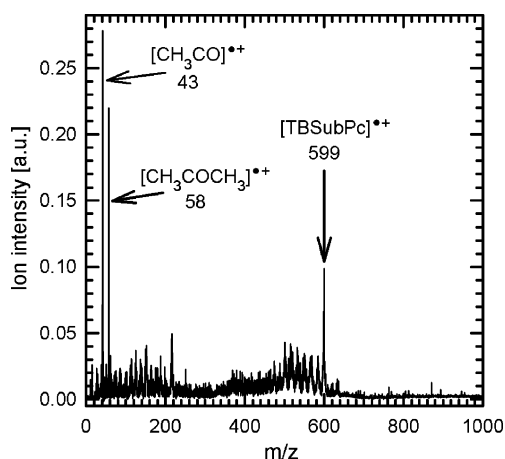


Figure 3. REMPI-TOFMS obtained using TBSuPc/acetone solution of 0.5 mM. Excitation wavelength was 310 nm. Measurement was performed using the molecular beam apparatus with the spray-jet technique.^{17–20}

ton ionization time-of-flight mass spectrum (REMPI-TOFMS) at an excitation wavelength of 310 nm (4.0 eV) obtained with the TBSuPc/acetone solution. Three strong peaks are visible in Figure 3; they were ascribed to a parent radical cation of TBSuPc $[\text{TBSuPc}]^{\bullet+}$ ($m/z = 599$), a radical cation of acetone $[\text{CH}_3\text{COCH}_3]^{\bullet+}$ ($m/z = 58$), and its fragment ion $[\text{CH}_3\text{CO}]^{\bullet+}$ ($m/z = 43$).²² The other smaller peaks were ascribed to fragment ions originating from $[\text{TBSuPc}]^{\bullet+}$. Fragment ions originating from a parent radical cation were frequently observed in our previous studies.^{17–20} This experimental result does not necessarily mean that the molecular species which are responsible for these small peaks were originally in the solution. Since the vertical ionization potential of TBSuPc is 6.243 eV according to a DFT calculation,²³ two-photon ionization of TBSuPc occurs under our experimental conditions. For the density-functional theory (DFT) calculation, the molecular geometry of TBSuPc was optimized using the Kohn–Sham DFT with the 6-31G* basis set and the Becke three-parameters hybrid exchange-correction functional known as B3LYP.²⁴ In the experiment, acetone and TBSuPc molecules were observed as individual molecules, and no clusters consisting of acetone and TBSuPc molecules were observed. We also confirmed that the

similar spectra in character are obtained for the TBSuPc/acetone solution between 0.1 mM to 1 mM.

In fact, this experiment was useful not only for obtaining information on molecular species in a molecular beam but also for optimizing the experimental conditions for the following molecular beam depositions. The main optimized parameters were the operation time and frequency of the pulsed nozzle. The relatively longer operation time of the pulsed nozzle were required so as to efficiently eject the solution mist in the inlet chamber into vacuum through the pulsed nozzle, while the frequency was adjusted so as to maintain high vacuum in the third chamber (C).

An STM image of the TBSuPc molecular overlayer deposited on the Au (111) using the spray-jet technique is shown in Figure 4a. Bright spots reflecting the protrusion of TBSuPc molecules as well as the herringbone reconstruction^{25,26} of the Au (111) surface can be seen. The TBSuPc molecules show a slight tendency to adsorb along the herringbone reconstruction of the Au (111) surface. A high-resolution image is shown in Figure 4b. The bright spots are attributable to *tert*-butyl groups bound to the periphery of the TBSuPc. A group of three spots can be assigned to an individual TBSuPc molecule. The image size of the TBSuPc is consistent with that previously reported.¹² The TBSuPc molecules tend to adsorb with the Cl pointing toward the substrate. This is due to the difference in interaction between the Cl and the Au substrate and between *tert*-butyl and the Au substrate; that is, the Cl atom has a stronger affinity to Au than *tert*-butyl groups, which is reasonable in consideration of static dipole induced in B–Cl bond.^{11,12} Some images of TBSuPc molecules do not form equilateral triangles in parts a and b of Figure 4 because TBSuPc includes four kinds of structural isomers, depending on the position of the *tert*-butyl groups.¹² Thus, we successfully obtained high-resolution STM images of TBSuPc deposited using our spray-jet technique, in which the *tert*-butyl groups of the TBSuPc molecules were identifiable.

Here, we should refer to the contaminants that can be seen in parts a and b of Figure 4. These appear at a relatively lower height in the STM images compared to the TBSuPc molecules, shown with arrows in Figure 4b. We found that the contaminants do not adsorb on the clean Au (111) surface during the transfer of the sample plate from the spray-jet molecular beam apparatus to the LT-STM. The following experiment was carried out for

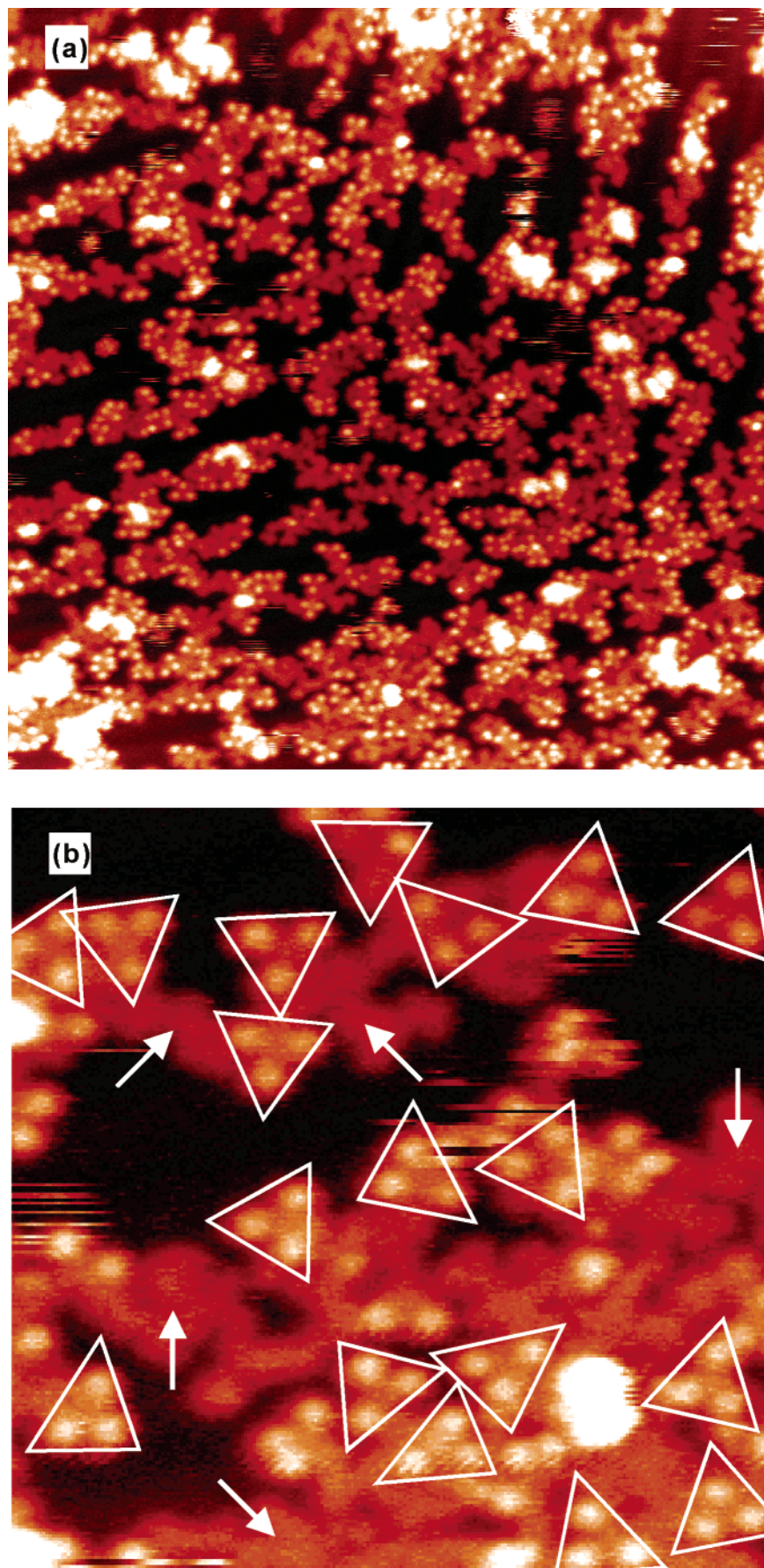


Figure 4. (a) STM image of molecular overlayer of TBSubPc molecules deposited by spray-jet technique on Au (111) surface and (b) magnified STM image. In (b), single TBSubPc molecules are represented by white triangles, while the contaminants are shown with white arrows. In both (a) and (b), *tert*-butyl groups in TBSubPc molecules are clearly identifiable. Image size = $70 \times 70 \text{ nm}^2$, $I_t = 20 \text{ pA}$, $V = 1.97 \text{ V}$ for (a). Image size = $17.5 \times 17.5 \text{ nm}^2$, $I_t = 20 \text{ pA}$, $V = 1.97 \text{ V}$ for (b).

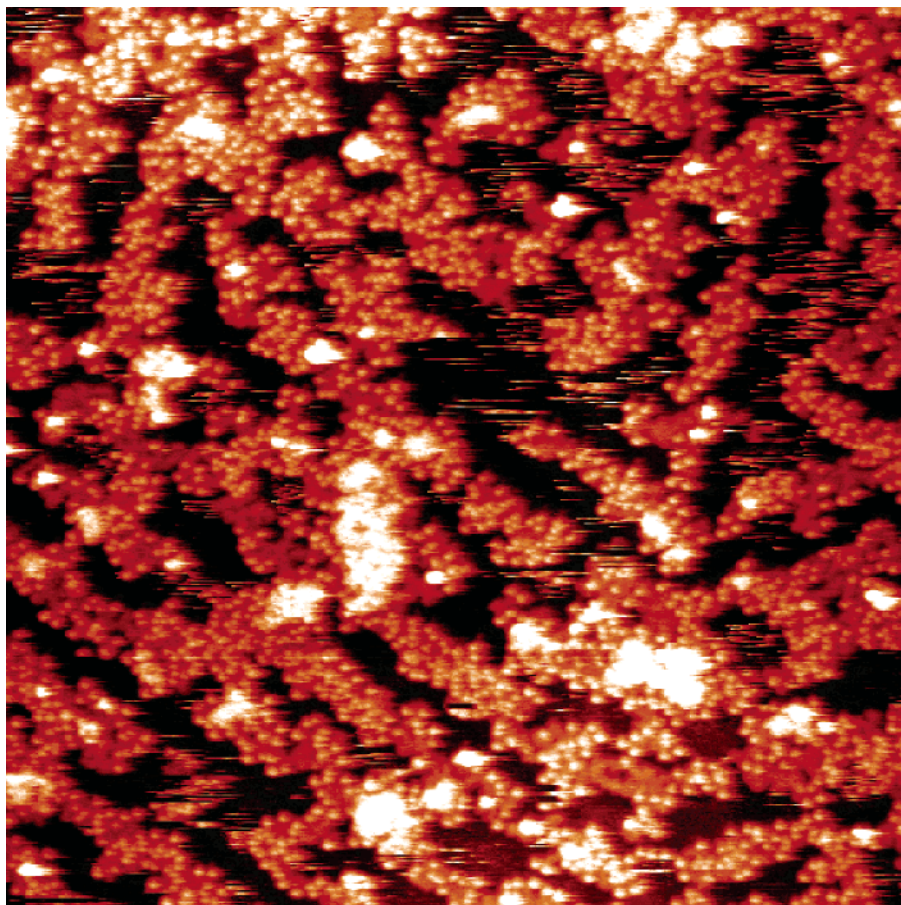


Figure 5. STM image of molecular overlayer of TBSuPc molecules at different positions of the same sample as shown in Figure 4. Image size = $70 \times 70 \text{ nm}^2$, $I_t = 20 \text{ pA}$, $V = 2.093 \text{ V}$.

the confirmation. The resident time of the clean Au (111) substrate in the transfer unit was adjusted to the resident time required for the transfer of the sample substrate deposited by the spray-jet technique; then the Au (111) substrate was transferred to the LT-STM, and the cleanness of the Au (111) surface was examined. The contaminants are therefore likely to originate from impurities in the acetone and/or from decomposed TBSuPc molecules. A small amount of contaminants that are similar in character were still observed on the clean Au (111) surface when a pure acetone solvent without the TBSuPc molecules was used as a sample solution in the spray-jet molecular beam deposition. This suggests that impurities in the acetone are at least one cause of the contamination. Furthermore, in recent preliminary experiments, the amount of contamination was considerably reduced when we used a chloroform solution for the spray-jet molecular beam deposition.²⁷ As TBSuPc is not dissolvable in chloroform, a chloroform solution of one of the porphyrin derivatives was used in the experiments. A special grade of chloroform (Wako Pure Chemical Industries, Ltd.) was used as the solvent.

These results indicate that the choice of solvent may be very important in reducing contamination. In future work, we will experiment with using various samples in different solvents, and this may produce interesting results.

We describe the characteristics of the spray-jet molecular beam deposition. We observed position-dependence in the concentration of the deposited TBSuPc molecules on the Au (111) surface. Figure 5 shows an STM image of molecular overlayer of the TBSuPc molecules on the Au (111) surface at different positions of the same sample. In this figure, there is a more dense concentration of TBSuPc molecules on the

Au (111) surface; individual TBSuPc molecules are visible as numerous bright spots, and their slight tendency to arrange themselves with a structure related to the herringbone reconstruction of Au (111) surface can be observed. We found that the spots of deposited molecules on the substrate are typically 4–6 nm in diameter and the concentration of the deposited molecules increases toward the center. This beam diameter was experimentally confirmed both by observing STM images at several positions in the sample by changing the position of the STM tip and by measuring absorption spectra at different positions in the sample. During the absorption measurements, the sample was exposed in air. The beam diameter is also consistent with the diameter obtained by calculating the solid angle of the molecular beam at the position β in Figure 2 that is determined by the geometry of our experimental setup, such as the position of the pulsed nozzle, the positions and the hole-diameters of the skimmers and the position of the sample plate.

Finally we describe the features of our technique compared to the pulse injection technique. The molecular beam deposition by spray-jet technique is performed at a relatively high vacuum. In the spray-jet technique, the generation of a molecular beam in high vacuum is achieved by the spray-jet inlet system, the double-skimmer structure that has a multiple stage differential pumping. Therefore the spray-jet technique enables us both to spectroscopically characterize the molecular species and to deposit molecular species in high vacuum. Knowing the information about the molecular beam helps to control the condition of the molecular beam deposition and further develop the spray-jet molecular beam deposition. Thus, compared to the pulse injection technique, the spray-jet technique is more analytical and sophisticated.

Conclusions

We developed a spray-jet molecular beam deposition apparatus. In combination with LT-STM, high-resolution STM images of TBSubPc molecules, in which *tert*-butyl groups were clearly identifiable in the TBSubPc molecules, were obtained, although there were some contaminants. These may have originated from impurities in the special grade of acetone used and/or from decomposed TBSubPc molecules. In relation to the characteristics of the spray-jet molecular beam deposition, we found that the spots of deposited molecules were typically 4–6 mm in diameter and there was a greater concentration of molecules toward the center.

In future work, further studies of various samples in different solvents should produce interesting results. In particular, this spray-jet technique could be applied to other molecular systems, such as nonsubimable molecules, thermally labile and/or reactive molecules, polymers, and biomolecules. A systematic study with our apparatus is in progress in our laboratory.²⁷

Acknowledgment. Dr. Ge would like to thank the Japan Society for Promotion of Science for a fellowship.

References and Notes

- (1) Chiang, S.; Wilson, R. J.; Gerber, Ch.; Hallmark, V. M. *J. Microsc.* **1988**, *152*, 567.
- (2) Chiang, S. *Chem. Rev.* **1997**, *386*, 1101.
- (3) Bai, C. *Scanning Tunneling Microscopy and its Application*; Springer-Verlag: Berlin, Heidelberg, Germany, 1995.
- (4) Meyer, E.; Hug, H. J.; Bennewitz, R. *Scanning probe microscopy*; Springer-Verlag: Berlin, Heidelberg, Germany, 2004.
- (5) Jung, T. A.; Schlittler, R. R.; Gimzewski, J. K. *Nature* **1997**, *386*, 696.
- (6) Gimzewski, J. K.; Joachim, C.; Schlittler, R. R.; Langlais, V.; Tang, H.; Johansson, I. *Science* **1998**, *281*, 531.
- (7) Moresco, F.; Meyer, G.; Rieder, K.-H.; Tang, H.; Gourdon, A.; Joachim, C. *Phys. Rev. Lett.* **2001**, *86*, 672.
- (8) Hipps, K. W.; Lu, X.; Wang, X. D.; Mazur, U. J. *J. Phys. Chem. B* **2000**, *104*, 11899.
- (9) Hipps, K. W.; Scudiero, L.; Barlow, D. E.; Cooke, M. P., Jr. *J. Am. Chem. Soc.* **2002**, *124*, 2127.
- (10) Yokoyama, T.; Yokoyama, S.; Kamidado, T.; Okuno, Y.; Mashiko, S. *Nature* **2001**, *413*, 619.
- (11) de Wild, M.; Berner, S.; Suzuki, H.; Yanagi, H.; Schlettwein, D.; Ivan, S.; Baratoff, A.; Guentherodt, H.-J.; Jung, T. A. *ChemPhysChem* **2002**, *3*, 881.
- (12) Suzuki, H.; Miki, H.; Yokoyama, S.; Mashiko, S. *J. Chem. Phys. B* **2003**, *107*, 3659.
- (13) Tanaka, H.; Hamei, C.; Kanno, T.; Kawai, T. *Surf. Sci.* **1999**, *432*, L611.
- (14) Kasai, H.; Tanaka, H.; Okada, S.; Oikawa, H.; Kawai, T.; Nakanishi, H. *Chem. Lett.* **2002**, *7*, 696.
- (15) Terada, Y.; Choi, B.-K.; Heike, S.; Fujimori, M.; Hashizume, T. *J. Appl. Phys.* **2003**, *93*, 10014.
- (16) Terada, Y.; Choi, B.-K.; Heike, S.; Fujimori, M.; Hashizume, T. *Jpn. J. Appl. Phys.* **2003**, *42*, 4379.
- (17) Yamada, T.; Shinohara, H.; Maofa, Ge; Mashiko, S.; Kimura, K. *Chem. Phys. Lett.* **2003**, *370*, 132.
- (18) Yamada, T.; Ge, M.; Shinohara, H.; Kimura, K.; Mashiko, S. *Chem. Phys. Lett.* **2003**, *379*, 458.
- (19) Yamada, T.; Shinohara, H.; Maofa, Ge; Kimura, K.; Mashiko, S. *Thin Solid Films* **2003**, *438–439*, 7.
- (20) Yamada, T.; Shinohara, H.; Maofa, Ge; Mashiko, S. *ITE Letter on Batteries, New Technologies & Medicine* **2004**, *5*, 358.
- (21) Chiba, T. *Ultrasonic Spray*; Sankaidou: Tokyo, Japan.
- (22) Majumder, C.; Jayakumar, O. D.; Vatsa, R. K.; Kulshreshtha, S. K.; Mittal, J. P. *Chem. Phys. Lett.* **1999**, *304*, 51 and references therein.
- (23) Frisch, M. J.; Trucks, G. W.; Schlegel, H. B.; Scuseria, G. E.; Robb, M. A.; Cheeseman, J. R.; Zakrzewski, V. G.; Montgomery, J. A., Jr.; Stratmann, R. E.; Burant, J. C.; Dapprich, S.; Millam, J. M.; Daniels, A. D.; Kudin, K. N.; Strain, M. C.; Farkas, O.; Tomasi, J.; Barone, V.; Cossi, M.; Cammi, R.; Mennucci, B.; Pomelli, C.; Adamo, C.; Clifford, S.; Ochterski, J.; Petersson, G. A.; Ayala, P. Y.; Cui, Q.; Morokuma, K.; Malick, D. K.; Rabuck, A. D.; Raghavachari, K.; Foresman, J. B.; Cioslowski, J.; Ortiz, J. V.; Stefanov, B. B.; Liu, G.; Liashenko, A.; Piskorz, P.; Komaromi, I.; Gomperts, R.; Martin, R. L.; Fox, D. J.; Keith, T.; Al-Laham, M. A.; Peng, C. Y.; Nanayakkara, A.; Gonzalez, C.; Challacombe, M.; Gill, P. M. W.; Johnson, B. G.; Chen, W.; Wong, M. W.; Andres, J. L.; Head-Gordon, M.; Replogle, E. S.; Pople, J. A. *Gaussian 98*, revision A.7; Gaussian, Inc.: Pittsburgh, PA, 1998.
- (24) Beche, A. D. *J. Chem. Phys.* **1997**, *104*, 242.
- (25) Wöll, Ch.; Chiang, S.; Wilson, R. J.; Lippel, P. H. *Phys. Rev. B* **1989**, *39*, 7988.
- (26) Barth, J. V.; Brune, H.; Ertl, G.; Behm, R. J. *Phys. Rev. B* **1990**, *42*, 9307.
- (27) Suzuki, H.; Yamada, T.; Kamikado, T.; Mashiko, S. Manuscript in preparation.